Egyptian Journal of Chemistry

http://ejchem.journals.ekb.eg/

Anti-Inflammatory Activity of Two new Acylic C18 Hydroxy Unsaturated Fatty Acids from The Gum Resin of *Styrax benzoin* in RAW264.7 macrophages

Mohamed H. Abd El-Razek,[a]* Tarik A. Mohamed,[b] Mohammed I. Ali,[c] Ahmed R. Hamed[b,d]*

[a]*Institute of Pharmaceutical Industries Research, Chemistry of Natural Compounds Department, National Research Center, 33 El-Buhouth St., Dokki, Giza 12622, Egypt.*

[b]*Chemistry of Medicinal Plants Department & Biology Unit Floor 6 CLN, National Research Centre, 33 El Bohouth St., Dokki, Giza 12622, Egypt.*

[c]*Medicinal and Aromatic Plants Research Department, National Research Centre, 33 El Bohouth St., Dokki, Giza 12622, Egypt.*

[d]*Biology Unit, Central Laboratory for Pharmaceutical and Drug Industries Research Institute, National Research Centre, 33 El Bohouth St., P.O. 12622, Dokki, Giza, Egypt*

Abstract

The phospholipid fatty acids composition of gum resin of *Styrax benzoin* was successively macerated with chloroform over 2 days. The exhaustively extracted at room temperature with $CHCl_3$ was evaporated to obtain the crude extract. Vacuum liquid column chromatography, thin layer chromatography and high performance liquid chromatography were performed to obtain two pure compounds. Both of compounds were elucidated and identified using the spectroscopic methods. We employed lipopolysaccharide (LPS)-induced nitric oxide inflammatory model in RAW264.7 macrophage cells. Successfully repeated chromatographic techniques with chemical methods resulted in purification and structure evaluation of two new C18 unsaturated hydroxy fatty acids from the gum resin of *Styrax benzoin*. Their structures were determined to be (3*R*,4*E*,6*E*)-3-Hydroxy-4,6-octadecadienoic acid (**1**) and (3*R*,9*E*,11*E*,15*E*)-13-Hydroxy-9,11,15-octadecatrienoic acid (**2**) according to different spectroscopic data. The configuration of ethylenic moiety were determined to be an *E*- stererostructures by comparison of coupling patterns of related proton signals in the ^{1}H-NMR and NOESY experiments. Other supporting results for the stereogenic centers for C-3 of compound (**1**) and C-13 of (**2**) by helping of Newman projection. Finally, the absolute stereochemical configuration was determined by using the modified Mosher method. Compound **2** showed a strong anti-inflammatory effect, as revealed by its concentration-dependent inhibition of LPS-induced NO release with IC_{50} of 13.5 µM.

***Keywords*:** Hydroxy fatty acids, *Styrax benzoin*, RAW 264.7 macrophages, Nitric oxide.

1. Introduction

Fatty acids (FAs) are considered the main source constituents of fats and oils. The chemical modification of both the carboxyl group and unsaturated hydrocarbon long chain centers present in FAs based on the industrial exploitation of oils and fats for food besides with oleochemical products. The presence of methylenes groups adjacent to the most reactive centers in FAs which are carboxylic group and double bonds moieties resulted in increasing their reactivity [1]. In general, the broadest common in nature of FAs which are the entirely straight chain aliphatic hydrocarbon carboxylic acids with length from C4 to C22 [1]. The stereomerism of the ethylenic bonds of unsaturated fatty acids (UFAs) can be either in *cis* or *trans* oriental of configuration [2]. Furthermore, the location of ethylenic unsaturated double bonds can be on different sides of the aliphatic straight chain resulting in positional isomers. According to this phenomena the *trans* fatty acids (TFAs) posses physico and chemical, nutritional, biochemical and biological properties are different from those of *cis* isomers (CFAs) [3]. Several studied have been done on the last three decades on TFAs showing their impact on human health and suspected to be harmful and a correlation between their ingestion for increasing of blood cholesterol level as well as the cardiovascular risks

*Corresponding author e-mail: abdelrazek3@yahoo.com; (Mohamed AbdEl-Razek),
n1ragab2004@yahoo.com; (Ahmed R. Hamed).
Receive Date: 10 February 2022; Revise Date: 28 February 2022; Accept Date: 13 March 2022.
DOI: 10.21608/ejchem.2022.120799.5434.

[3]. In the geometrical stereoisomers TFAs have a spatial configuration that is halfway between that of SFAs and *cis* unsaturated fatty acids (CUFAs), as well as the double bonds angle of TFAs is smaller compared to the *cis* isomeric, and the acyl chain is more linear, resulting in a stiffer and straighter molecule with a higher melting point [3]. As a result of the presence of *trans*-double bonds, the physical properties of FAs are more comparable to those of saturated than UFAs. Oxidation, elongation, and desaturation processes can all be used to break down the cis-trans isomers of fatty acids [3].

In recent research, we assessed the antibacterial activity of six triterpenes extracted from the chloroform ($CHCl_3$) extract of *Styrax benzoin* gum resin (Styracaceae). Based on these findings, it has been shown that *S. benzoin* can be utilised as a possible source of antibacterial compounds [4]. In a point of view the medicinal potential of *S. Benzoin*, we continuously examined the low soluble fraction from the chloroform extract. Inflammation is implicated in the occurrence and progression of many diseases such as cancer, cardiovascular disorders, diabetes and neurological disorders [5-7]. There is a demand for an effective natural drug that interferes with inflammatory reactions. Therefore, in the present study, we investigated the potency of the two isolated compounds to inhibit the inflammatory mediator nitric oxide in RAW264.7 macrophage cells.

2. Experimental

2.1. Reagents and apparatus

Melting points were determined using a Yanagimoto micro-melting point apparatus and are uncorrected. IR spectra were measured on a Mattson Genesis II spectrophotometer. The optical rotation was determined on a Perkin-Elmer Model 341 Polarimeter. Low resolution EIMS were collected on a Joel JMS-SX/SX 102A mass spectrometer at 70 eV. NMR spectra were obtained on a Bruker-500 FT NMR spectrometer. Chemical shifts were expressed in δ (ppm) relative to the solvent signal as internal standard and coupling constants (*J*) were given in hertz. TLC was carried out on precoated Silica gel 60 F_{254} (Merck, art. 5715). Column chromatography was performed on Silica gel 60 (Merck, 40-63 and 63-200 μm), Sephadex LH-20 (Sigma, 25-100 μm) and (HPLC) was carried out a JASCO PU-980 apparatus equipped with a JASCO UV-970 detector. Hypersil ODS 5 μm (250 × 4.6 mm i.d.) and preparative ODS 5 μm (250 × 21.2 mm i.d.) columns were used for analytical and preparative purposes.

2.2 RAW 264.7 Cell Culture

Murine macrophages RAW264.7 cells (ATCC®) were maintained in complete Dulbecco's Modified Eagle's Medium (DMEM, Corning, USA) supplemented with 10% fetal bovine serum, penicillin (100 U/mL), streptomycin sulphate (100 μg/mL) and 2 mM L-glutamine in a humidified 5% CO_2 incubator. For passaging and treatment, cells were washed with phosphate buffered saline and scrapped off the flasks using sterile scrappers (SPL, Spain).

2.3 Inhibition of LPS-induced NO release

Model of inhibition of LPS-induced NO release in RAW 264.7 macrophages was performed as previously published [8]. Briefly, cells (0.5×10^6 cells/mL) were seeded onto 96-well microwell plates and incubated for 24 h. At the next day, non-induced quadruplicate wells received medium with the vehicle (DMSO, final concentration =0.1% *v/v*). Inflammation group of quadruplicate wells received lipopolysaccharide (LPS) as 100 ng/mL in complete culture media and 0.1% DMSO, by volume]. Compound groups of quadruplicate wells received increasing concentrations (6.25-100 μM) of the compound dissolved in DMSO and diluted into culture media containing LPS. Caffeic acid phenethyl ester (CAPE, 5 μM) was used as a routine anti-inflammatory positive control for the assay. After 24 h of incubation, Griess assay was used to determine NO in all wells. Equal volumes of culture supernatants and Griess reagent were mixed and incubated at room temperature for 10 min and read at absorbance of 520 nm on a Tristar^{2}lb™ microplate reader (Berthold, Germany). NO Inhibition % of test extract was calculated relative to the LPS-induced inflammation group, normalized to cell viability determined with Alamar Blue™ reduction assay [9]. IC_{50} was calculated on GraphPad prism (San Diego, USA) using non-linear regression analysis.

2.4. Plant material and sample preparation

The gum of *Styrax benzoin* Dryand., 'Jurur', was a chocolate brown coloured resin with some lighter areas, the particle size was about 1 cm^3. The resin was harvested from the outside of the bark and therefore, exposed to light for several days. It was imported from India and obtained from El-Gomhouria Co., for Drugs and Equipments, 13-Mahmoud Basuny St., El-Tahrir Sq., Cairo, Egypt.

2.5. Extraction and isolation

The gum resin of *S. benzoin* (500 g) was exhaustively extracted at room temperature with $CHCl_3$ over 2 days. After filtration the combined extracts (6 L) were evaporated under reduced

pressure to give 150 g of a brown oily material. 20 g of this oily residue were chromatographed over silica gel using a *n*-hexane/ $CHCl_3$ and a $CHCl_3$/ MeOH gradient to get thirty-six fractions. Fractions were combined based on their TLC pattern to yield subfraction designated as SB1-SB6. Subfraction SB1 (500 mg) was chromatographed over silica gel eluting with *n*-hexane/EtOAc (97:3) to get a yellow oil (399 mg) which was applied to a Sephadex LH-20 column and eluted with hexane-CH_2Cl_2-MeOH (2:5:1) to yield of a strongly UV-active mixture (280mg). Final preparative separation was accomplished by (HPLC) (Diol, 7 µm, 1 × 25 cm, 50 mL/min, monitored @ 258 nm, hexane EtOAc, 9:1) and C18 (8 µm, 1 × 25 cm, MeOH-H_2O, 4:1) to yield (81 mg) of compound **1** and (88 mg) of **2**.

2.5.1 Preparation of (*S*)- and (*R*)-MTPA Esters (1a, 1b, 2a and 2b) of compounds 1 & 2.

To a solution of **1** and **2** (2 mg in 0.5 ml of pyridine) was added *S*-(+)- or *R*-(-)-MTPA chloride (one drop) and the solution was allowed to stand at room temperature for 7 h. After purification using TLC, the ester of **1** (1.6 mg, 80% yield) and of **2** (1.55 mg, 77.5 %) were analyzed by ^{1}HNMR spectroscopic measurement and $\Delta\delta = \delta_S - \delta_R$ was calculated for **1** and **2**.

2.5.2.(3*R*,4*E*,6*E*)-3-Hydroxy-4,6-octadecadienoic acid (1)

Obtained as colorless oil (81 mg); m.p = 58.5 ^{o}C; $[\alpha]_D^{25}$ = + 11.1 ($CHCl_3$, *c*=1.33) ; UV (MeOH, log ε) λ_{max}: 260 (3.78), 272 (3.56), 283 (3.59); IR ($CHCl_3$) ν_{max} : 3566, 3390, 2928, 2855, 1709, 1412, 1248, 990, 966; EI-MS *m/z* (relative intensity) [M^+] 296 (14), 207 (30) [M-$CHOHCH_2COOH$]$^+$, 181 (40), 29 (60) see Figure **3**; HREI-MS *m/z* 296.2034 [M+] (Calcd. 296.1946 for $C_{18}H_{32}O_3$); ^{1}H-NMR (500 MHz, $CDCl_3$): see Table **1**; ^{13}C-NMR (125 MHz, $CDCl_3$): see Table **1**. On the basis of spectroscopic analyses, the structure of the isolated secondary metabolite was determined as shown in Figure **1**.

2.5.3.(*S*)-1a: ^{1}H-NMR ($CDCl_3$, 500 MHz)

δ_H 6.60 (1H, td, *J* = 16.0, 2.0 Hz; H-5), 6.00 (1H, t, *J* = 16.0 Hz; H-6), 5.75 (1H, dd, *J* = 16.0, 12.0 Hz; H-4), 5.59 (1H, ddd, *J* = 16.0, 12.0, 7.0 Hz; H-7), 5.40 (1H, dddd, *J* = 12.0, 9.0, 7.0, 2.0 Hz; H-3), 2.52 (1H, dd, *J* = 14.0, 9.0 Hz; H-2_a), 2.44 (1H, dd, *J* = 14.0, 7.0 Hz; H-2_b).

2.5.4.(*R*)-1b: ^{1}H-NMR ($CDCl_3$, 500 MHz)

δ_H 6.65 (1H, td, *J* = 16.0, 2.0 Hz; H-5), 5.98 (1H, t, *J* = 16.0 Hz; H-6), 5.78 (1H, dd, *J* = 16.0, 12.0 Hz; H-4), 5.60 (1H, ddd, *J* = 16.0, 12.0, 7.0 Hz; H-7), 5.46 (1H, dddd, *J* = 12.0, 9.0, 7.0, 2.0 Hz; H-3), 2.52 (1H, dd, *J* = 14.0, 7.0 Hz; H-2_b), 2.38 (1H, dd, *J* = 14.0, 9.0 Hz; H-2_a).

2.5.5.(*13R,9E,11E,15E)*-13-Hydroxy-9,11,15-octadecatrienoic acid (2)

Obtained as yellow oil (88 mg); m.p = 61.5 ^{o}C; $[\alpha]_D^{25}$ =+19.2 ($CHCl_3$, *c*= 0.9); UV (MeOH, log ε) λ_{max} 240 (3.52), 260 (3.44), 269 (3.87), 283 (3.29); IR ($CHCl_3$) ν_{max} : 3656, 2925, 2854, 1712, 1463, 1259, 990, 966; EI-MS *m/z* (relative intensity) [M^+] 294 (20), 143 (14) [M-$(CH_2)_7COOH$]$^+$, 151 (22), 125(30), 99 (60), 55 (40), 29 (60) see Figure **3**; HREI-MS m/z 294.2021 [M+] (Calcd 294.1933 for $C_{18}H_{30}O_3$); ^{1}H-NMR (500 MHz, $CDCl_3$): see Table **2**; ^{13}C-NMR (125 MHz, $CDCl_3$): see Table **2**. Based on the spectroscopic analyses, the structure of the isolated metabolite was determined as shown in Figure **1**.

2.5.6.(*S*)-2a: ^{1}H-NMR ($CDCl_3$, 500 MHz)

δ_H 6.58 (1H, t, *J* = 16.0 Hz, H-11), 5.77 (1H, dt, *J* = 12.0, 7.0 Hz, H-13), 5.70 (1H, dd, *J* = 16.0, 12.0 Hz, H-12), 5.53 (1H, ddd, *J* = 16.0, 12.0, 7.0 Hz, H-16), 5.37 (1H, ddd, *J* = 16.0, 12.0, 8.0 Hz, H-15), 2.55 (2H, m, H-14).

2.5.7.(*R*)-2b: ^{1}H-NMR ($CDCl_3$, 500 MHz)

δ_H 6.60 (1H, t, *J* = 16.0 Hz, H-11), 5.82 (1H, dt, *J* = 12.0, 7.0 Hz, H-13), 5.72 (1H, dd, *J* = 16.0, 12.0 Hz, H-12), 5.54 (1H, ddd, *J* = 16.0, 12.0, 7.0 Hz, H-16), 5.38 (1H, ddd, *J* = 16.0, 12.0, 8.0 Hz, H-15), 2.50 (2H, m, H-14).

3. Results and discussion

Different reliable tools of chromatographic analysis led to the isolation of two new secondary metabolites UHFAs from the gum resin of *S. Benzoin*. The structures of compounds **1** and **2** (Figure **1**) were deduced from all the spectroscopic data including UV, IR, MS and 2D-NMR (Tables **1**& **2**).

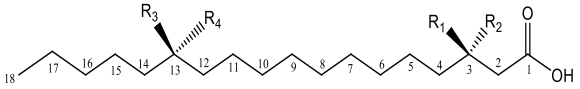

(**1**) $R_1 = R_3 = R_4 = H$, $R_2 = OH$, $\Delta^{4,6}$
(**2**) $R_1 = R_2 = R_4 = H$, $R_3 = OH$, $\Delta^{9,11,15}$

Figure 1. Chemical structures of hydroxy unsaturated fatty acids **1** and **2.**

As revealed by the Griess assay, compound **2** showed a strong concentration-dependent inhibition of LPS-induced NO release from RAW264.7 macrophages. In contrast, compound **1** showed weak concentration-dependent inhibition of NO release.

IC_{50} of compound **2** was statistically derived from GraphPad Prism software and was found to be 13.5 µM.

Compound **1** was obtained as colourless oil with low melting point at 58.5 °C besides the chirality active centre which had an optical rotation $[\alpha]_D^{25}$ = + 11.1 ($CHCl_3$, *c* =1.33). HREI-MS found the chemical formula of **1** as $C_{18}H_{26}O_2$, with a molecular ion peak at *m/z* 296.2034 (Calcd. 296.1946), showing three degrees of unsaturation. The existence of diagnostic hydroxyl groups (3566, 3390 cm^{-1}), aliphatic carbons (2928, 2855 cm^{-1}), carboxylic acid band at 1709 cm^{-1}, and an olefinic band at 1643 cm^{-1} was suggested by the IR bands. The UV peaks λ_{max} (MeOH) at 229, 240, 260, 272, 283 and the absorption bands at (990, 966 cm^{-1}) were used to infer the presence of conjugated unsaturated bonds in an *E*-configuration [10-12]. Careful investigation of ^{13}C-NMR (Table **1**), DEPT and HMQC spectra presented that **1** possessing 18 carbon signals, including characteristic signals due to one carboxyl (δ_C 179.3), four sp^2 CH olefinic methines (δ_C 135.7, 132.7, 127.9, 125.8), one sp^3 oxygenated methine (δ_C 72.2), eleven sp^3 methylenes (δ_C 34.1, 31.9, 29.3, 28.4 (x6), 25.6, 22.5), two of them which at δ_C 34.1, 25.6 due to an envelope methylenes, two downfield methylene groups (δ_C 31.9, 29.3) and at the end one terminal methyl (δ_C 14.2) indicating that **1** belongs to C18 fatty acid containing secondary alcoholic methine along with two double bonds in the presence of a terminal carboxyl group. The presence of seven spin systems was discovered during preliminary inspection of ^{1}H NMR (Table **1**) and ^{1}H-^{1}H COSY spectra, as illustrated in Figure **2**. An envelope downfield methylene protons at (δ_H 2.34 dd, *J* = 14.0, 9.0 Hz; 2.27 dd, *J* = 14.0, 7.0 Hz, H_2-2) which are α-position to the terminal carboxylic group showed a COSY correlation to the proton of oxymethine, putting at C-3 (δ_H 4.10 dddd, *J* = 12.0, 9.0, 7.0, 2.0 Hz; δ_C 72.2) seems to be at β-position to the carbonyl carbon of the terminal carboxyl group. This evidence was supported by $^2J_{CH}$ correlation in the HMBC (Table **1**) spectrum towards the carbonyl carbon (δ_C 179.3, C-1) and proton of oxymethine (δ_C 72.2, C-3). The fragment at *m/z* 207 in EI-MS (Figure **3**) established the connection of an envelope methylene protons and oxymethine proton to be an α,β-position to the carbonyl carbon of the terminal carboxyl group. The existence of a conjugated unsaturated bonds was inferred from a COSY (Figure **2**). correlation of disubstituted olefinic proton (δ_H 5.66 dd, *J* = 16.0, 12.0 Hz; H-4) to the oxymethine proton placing at C-3 (δ_H 4.10 dddd, *J* = 12.0, 9.0, 7.0, 2.0 Hz; H–3) and with another olefinic protons (δ_H 6.52 td, *J* = 16.0, 2.0 Hz; H-5). The more downfield olefinic proton H-5 (δ_H 6.52) had a correlation in COSY spectrum (Figure **2**) with the other ethylenic proton (δ_H 5.99 t, *J* = 16.0 Hz; H–6), which in turn couples to H-7 (δ_H 5.53 ddd, *J* = 16.0, 12.0, 7.0 Hz).

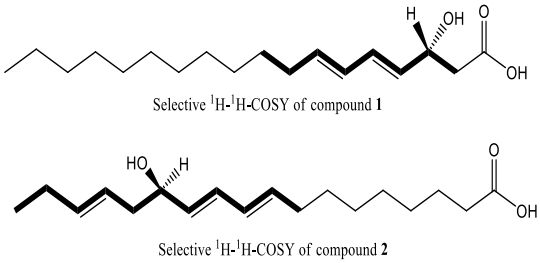

Figure 2. Two-dimensional NMR spectrum of new fatty acids **1** and **2.**

The small coupling constant (*J* = 2.0 Hz) was resulting from allylic long range between the oxymethine proton at C-3 and the disubstituted ethylenic proton H-5. From the fragments at *m/z* 155 in EIMS (Figure **3)**, established the skeleton positions of the olefinic four protons [13-16]. Furthermore H-4 (δ_H 5.66) showed $^2J_{CH}$ correlation with (δ_C 125.8, C-5) and secondary alcoholic carbon (δ_C 72.2, C-3) along with $^3J_{CH}$ correlation with an envelope methylene (δ_C 34.1, C-2) and the carbon signal (δ_C 127.9), which was attributed to the third olefinic carbon C-6. According to these evidence, H-4 should be γ-position to the carbonyl carbon of the carboxyl group.

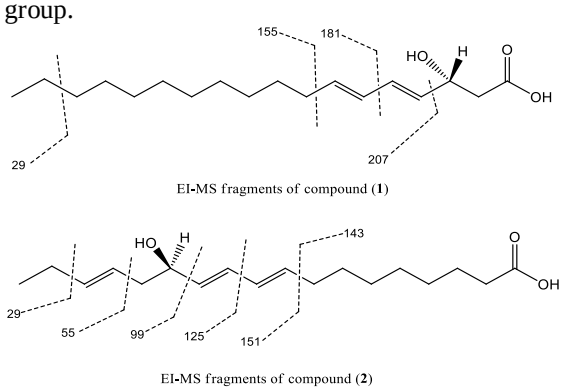

Figure 3. The essential fragment ions for compounds (**1**) and (**2**).

HMBC correlations between the last olefinic proton (δ_H 5.53 ddd, *J* = 16.0, 12.0, 7.0 Hz; H–7) and carbon signals (δ_C 125.8, C-5), (δ_C 29.3, C-9) permitted the placement of ene-ene unit is connected to a carboxylic acid function *via* an oxymethine carbon (C-3) and an envelope methylene carbon (C-2). As H-6 appeared as a triplet and H-5 as a double of doubles with a big coupling constant (*J* = 16.0 Hz) in the ^{1}H NMR spectrum and these values gives us the

confidence that we are dealing with stereoisomerism with an *E*-configuration. H-7 (δ_H 5.53 ddd, J = 16.0, 12.0, 7.0 Hz) gave a correlation with (δ_H 2.25m; H_2-8) and then linked to the methylene envelope at (H 1.30 m; H_2-9) in the COSY spectrum, showing the start of the alkyl chain. Based on the results of mass spectrometry for this molecule, the alkyl chain was discovered to have ten methylene groups and a terminal methyl group (Figure **3**). Terminal methyl group (δ_H 0.80 t, J = 7.2 Hz, H_3-18) coupled into the methylene envelope (δ_H1.32 m; H_2-17) in the COSY spectrum. A NOSY spectrum was used to establish **1**'s relative configuration (Figure **4**). Figure **1** shows the NOESY correlations between H-3/H-2, H-5; H-5/H-7 and H-4/H-6, H-2, which suggested the relative configuration of **1**. The NMR spectroscopic data of **1** were also compared to those of (ζ)-3-hydroxy-octadeca-4(*E*),6(*Z*)-dienoic acid, which was previously reported from *Scrophularia deserti* by Stavri M. et al., [17], leading to the conclusion that the structure of 1 has the same planar structure as (ζ)-3-hydroxy-octadeca-4(*E*),6(*Z*)-dienoic acid. The distinct rotational differences and NMR data clearly proved that they are diastereomers. Upon the previous NMR data and the other physical properties data of **1**, our attention was directed to the vicinal coupling constant by the methine secondary alcoholic proton (δ_H 4.10 dddd, J = 12.0, 9.0, 7.0, 2.0 Hz; H–3), which performs a coupling with the olefinic proton H-4 and H_2-2 along with H-5 cross allylic long range. All the above vicinal coupling of H-3 was clearly confirmed by cross peaks in the ^{1}H-^{1}H COSY

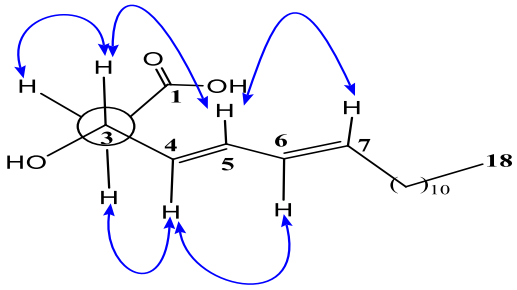

Figure 4. The key NOESY correlations and Newman projection of **1.**

spectrum (Figure **2**). Careful examination of Dreiding models demonstrated than in a conformation maintaining the co-planarity of the carbonyl carbon of the carboxyl group, along with one of vicinal envelope methylene protonsbesides the allylic proton H-5and the methine proton (H-3), assume that the previously protons (H-3, H-2 and H-5) lie on the same side with the terminal carboxylic group as shown in Figure **4** (Newman projection). These observed vicinal coupling constants can be predicted by the Karplus Conroy relationships (dihedral angles involving H-3, H-2 and H-5). Moreover, Newman projection answers the question of the absence of the intramolecular hydrogen bond signal in the ^{1}H-NMR spectrum as the terminal carboxylic group and the -OH does not share the coplanarity and laying at opposite side (Figure **4**). The optical rotation for **1** was rotation $[\alpha]_D^{25}$ = + 11.1 ($CHCl_3$, c =1.33), which can be considered that make sense that **1** is not a kind of racemic mixture. However, if **1** resulted from the biosynthesis *via* non-enzymatichydrolysis of a 2–3 double bond where attack by a water molecule from both faces of the olefin would lead to a racemate (Figure **5**). Using Mosher's ester technique [18], an attempt was made to assign the absolute stereochemistry of compound **1** at the C-3 position. Through the use of Mosher techniques, it is possible to upgrade the relative configuration setup to an absolute one. To do this, two aliquots of **1** were treated in dry pyridine with (*R*)- and (*S*)-MTPA chloride to yield the corresponding (*S*)-**1a** and (*R*)-**1b** MTPA esters. The pattern of (*S*-*R*) values (+0.18, +0.08, +0.04, -0.03, +0.05, -0.02, and +0.01 for H-2, H-3, H-4, H-5, H-6, and H-7, respectively) established the *R*-configuration at C-3, allowing the stereostructure of **1** to be assigned as (3*R*,4*E*,6*E*)-3-Hydroxy-4,6-octadecadienoic acid.

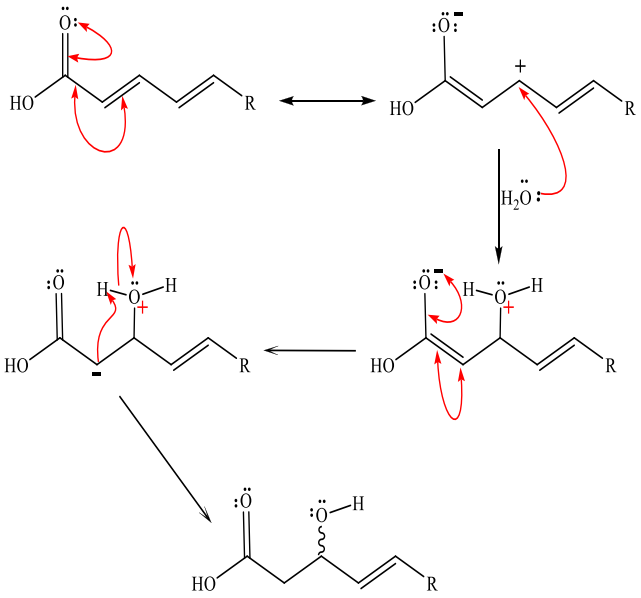

Figure 5. Suggested biosynthesis of **1.**

The second peak eluting from the preparative HPLC appeared to contain the second novel UHFAs. Subsequent C18 HPLC yielded compound **2** as yellow oil that analyzed for $C_{18}H_{30}O_3$ by HREIMS. Compound **2** had a melting point at 61.5 °C with a specific rotation of $[\alpha]_D^{25}$ = +19.2 ($CHCl_3$, c = 0.9). The structure of **2** was established based on analysis

of ^{1}HNMR, ^{13}CNMR, DEPT, ^{1}H-^{1}H COSY, HMQC, HMBC, NOSY, EIMS and HREIMS. The new metabolite **2** exhibited physical and spectral features similar to those of **1**. The calculated index of Hydrogen deficiency of the molecule is four and comparison with **1**, which had a three degree of unsaturation confirmed that **2** is less than **1** by 2 amu arising that **2** has one more double bond. Furthermore, compound **2** differ from **1** in the arrangement of disubstituted three double bonds and the position of a carbonilic carbon atom.^{13}C NMR (Table **2**) of compound **2** also revealed the presence of three double bonds and a secondary hydroxyl group as a part of the main skeleton of the molecule.^{13}CNMR spectrum of **2** exhibited one carboxyl (δ_C 179.6), six olefinic methines (δ_C 123.7, 125.9, 127.9, 132.9, 134.9, 135.1), one oxygenated methine (δ_C72.1), nine methylenes (δ_C20.7, 27.5, 29.3 (x5), 35.2, 37.2) and terminal methyl (δ_C 14.2) carbon signals, indicating that **2** has to be an acyclic C18 fatty acid containing three double bonds and ahydroxyl group. This result was confirmed by its molecular weight by HREI-MS m/z 294.2021 [M^+] (Calcd for 294.1933). Further information on the structure of an alkene-ol chain of **2** was obtained from analysis of the ^{1}H NMR spectrum. In addition to, the ^{1}HNMR spectrum of **2** (Table **2**), indicated that the presence of one terminal methyl (δ_H1.00 t, J = 7.3 Hz; H_3–18), six disubstituted olefinic methines (δ_H 5.51 ddd, J = 16.0, 12.0, 7.0 Hz, H-9), (δ_H 5.96 t, J = 16.0 Hz, H-10), (δ_H 6.55 t, J = 16.0 Hz, H-11), (δ_H 5.65 dd, J = 16.0, 12.0 Hz, H-12), (δ_H 5.36 ddd, J = 16.0, 12.0, 8.0 Hz, H-15), (δ_H 5.53 ddd, J = 16.0, 12.5, 8.0 Hz, H-16), one oxygenated methine (δ_H 4.31 dt, J = 12.1, 7.0 Hz, H-13) and nine methylenes, five of them (δ_H 1.29 m, 10H), one was adjacent to the terminal carboxyl group (δ_H 1.51 m, H_2-2) along with three allylic methylenes (δ_H 2.19 m, H_2-8), (δ_H 2.34 m, H_2-14) and (δ_H 2.06 m, H_2-17) signals were observed. An *E*-configuration for these three double bonds was suggested by the 16.0 Hz coupling constant for the ethenlyic protons. By comparing ^{I}H-NMR (Table **2**) and^{13}C-NMR (Table **2**) data of **2** to those of **1** it is reasonable to say that **2** possessed the structure of **1** except the arrangement of function groups with one more double bond. COSY spectrum (Figure **2**) also showed a separate spin system that began at the allylic hydroxy bearing methine (δ_H 4.31) was coupled to a *trans*-olefin resonance (δ_H 5.65 H-12), which, in turn was coupled to its vicinal partner (δ_H 6.55 H-11). A correlation was observed between this latter signal (δ_H 4.31 H-13) and an allylic methylene (δ_H 2.19). In the spin system associated with the terminal olefin, the proton at (δ_H 5.53 H-16) was *trans* coupled to a proton at (δ_H 5.36 H-15) and vicinally coupled to an allylic methylene at δ_H 2.06 (H_2-17). This spin system also correlated to the methylene envelope δ_H 2.06 (H_2-17) to other terminal disubstituted olefinic proton at (δ_H5.51 H-9) which showed a *trans* coupling with (δ_H 5.96 H-10). After the ^{13}C resonances had been assigned by HMQC (see Table **2**), partial structures were linked using an HMBC experiment (Table **2**). key correlations included $^{2}J_{CH}$ those observed between the carbinol proton at (δ_H 4.31 H-13) and C-14 (δ_C 35.2) in addition to C-12 (δ_C 134.9). A $^{3}J_{CH}$ between the δ_H2.34 methylene and (δ_C 134.9 C-12; δ_C 135.1 C-16) resonance firmly placed the carbinol at δ_C 72.1 vicinal to the C-14 and C-12. On the opposite side of the diene spin system was observed acorrelation between (δ_H 4.31) the carbinol proton and (δ_C 125.9 C-11 and 123.7 C-15), as well as a $^{3}J_{CH}$ between δ_H 5.65 (H-12) and δ_C 127.9 (C-10). The same proton H-11 Showed $^{2}J_{CH}$ with C-12 and C-10, as well as $^{3}J_{CH}$ with δ_C 132.9 (C-9) and δ_C 72.1 (C-13). This evidence enhancement to place the carbinol carbon and internal methylene carbon in between the interior diene and the external double bond. The presence of the peaksat *m/z* = 151 [M-$(CH_2)_7CO_2H$]$^+$ and *m/z* = 143 which represents the other fragment [M-$(CH{=}CH)_2$ $CHOHCH_2CHCHCH_2CH_3$]$^+$ (see Figure **3**), further showed that the ene-ene-($CHOHCH_2$)-ene unit is connected to a carboxylic acid function by seven methylene groups. By comparing ^{I}H-NMR (Table **2**) and^{13}C-NMR (Table **2**) data of **2** to those of 13-hydroxy-9*Z*,11*E*,15*E*-octadecatrienoic acid which was previously reported from the leaves of *Cucurbita moschata* [19].

It seems that **2** is a steroisomer of the reported one. At the reported one the orientation of the hydroxy group was not clear. The relative configuration of **2** was determined by the aid of a NOSY spectrum (Figure **6**). The NOESY correlations

Table 1. Chemical shift data of proton (500 MHz, $CDCl_3$), carbon (125 MHz, $CDCl_3$), and heteronuclear multiple bond correlation of **1.**

Position	^{13}C-NMR	^{1}H-NMR	Key HMBC correlations	
		δH (*J* in Hz)	^{2}J	^{3}J
1	179.3	----------		
2a	34.1	2.34 (1H, dd, *J* = 14.0, 9.0 Hz)	C-1, C-3	C-4
2b		2.27 (1H, dd, *J* = 14.0, 7.0 Hz)	C-3	
3	72.2	4.10 (1H, dddd, *J* = 12.0, 9.0, 7.0, 2.0 Hz)	C-2, C-4	C-1, C-5
4	135.7	5.66 (1H, dd, *J* = 16.0, 12.0 Hz)	C-3, C-5	C-2, C-6
5	125.8	6.52 (1H, td, *J* = 16.0, 2.0 Hz)	C-4, C-6	C-3, C-7
6	127.9	5.99 (1H, t, *J* = 16.0 Hz)	C-5	C-4, C-8
7	132.7	5.53 (1H, ddd, *J* = 16.0, 12.0, 7.0 Hz)	C-6, C-8	C-5, C-9
8	25.6	2.20 (2H, m)		
9	29.3	1.30 (2H, m)		
10	28.4	1.30 (2H, m)		
11	28.4	1.30 (2H, m)		
12	28.4	1.30 (2H, m)		
13	28.4	1.30 (2H, m)		
14	28.4	1.30 (2H, m)		
15	28.4	1.30 (2H, m)		
16	31.9	1.30 (2H, m)		
17	22.5	1.32 (2H, m)		
18	14.2	0.80 (3H, t, *J* = 7.2 Hz)	C-17	C-16

Table 2. Chemical shift data of proton (500 MHz, $CDCl_3$), carbon (125 MHz, $CDCl_3$), and heteronuclear multiple bond correlation of **2.**

Position	^{13}C-NMR	^{1}H-NMR	Key HMBC correlations	
	δC	δH (*J* in Hz)	^{2}J	^{3}J
1	179.6	----------		
2	37.2	1.51 (2H, m)	C-1	C-4
3	29.3	1.29 (2H, m)		
4	29.3	1.29 (2H, m)		
5	29.3	1.29 (2H, m)		
6	29.3	1.29 (2H, m)		
7	29.3	1.29 (2H, m)		
8	27.5	2.19 (2H, m)		
9	132.9	5.51 (1H, ddd, *J* = 16.0, 12.0, 7.0 Hz)	C-8	C-11
10	127.9	5.96 (1H, t, *J* = 16.0 Hz)	C-9	C-8, C-12
11	125.9	6.55 (1H, t, *J* = 16.0 Hz)	C-10	C-9, C-13
12	134.9	5.65 (1H, dd, *J* = 16.0, 12.0 Hz)	C-11, C-13	C-10, C-14
13	72.1	4.31 (1H, dt, *J* = 12.0, 7.0 Hz)	C-12, C-14	C-11, C-15
14	35.2	2.34 (2H, m)	C-13, C-15	C-12, C-16
15	123.7	5.36 (1H, ddd, *J* = 16.0, 12.0, 8.0 Hz)	C-14	C-13, C-17
16	135.1	5.53 (1H, ddd, *J* = 16.0, 12.0, 7.0 Hz)	C-15	C-14, C-18
17	20.7	2.06 (2H, m)	C-16, C-18	C-15
18	14.2	1.00 (3H, t, *J* = 7.2 Hz)	C-17	C-16

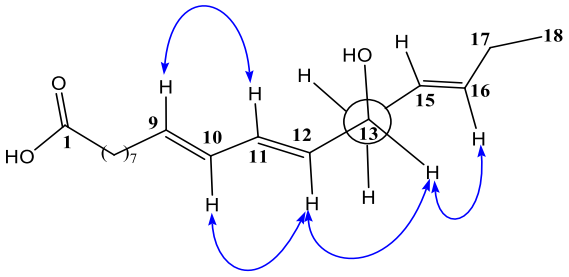

Figure 6. The key NOESY correlations and Newman projection of **2.**

between H-13/H-12,H-16; H-12/H-10; H-1/H-9 suggested the relative configuration of **2** as shown in Figure **1**. Careful examination of Dreiding models demonstrated than in a conformation maintaining the coplanarity of the methine carbonilic carbon (H-13) and the spin system of terminal group ($CH=CHCH_2CH_3$), assume that the previously protons (H-13, H-5 and H-6) lie on the same side with the terminal Me-18 group as shown in Figure **6** (Newman projection). These observed vicinal coupling constants can be predicted by the Karplus Conroy relationship (dihedral angles involving H-13, H_2-14 and H-12). A trial was made to assign the absolute stereochemistry at the C-13 position for compound **2** using Mosher's ester methodology [10]. The possibility of upgrading the above relative configuration to the absolute one, through application of the Mosher methods. For this aim, two aliquots of **2** were treated with (*R*)- and (*S*)-MTPA chloride in dry pyridine to give the corresponding (*S*)-**2a** and (*R*)-**2b** MTPA esters. The pattern of Δδ (*S*-*R*) values (-0.02, +0.02, +0.05, +0.05, -0.01 and -0.01 for H-11, H-12, H-13, H-14, H-15 and H-16 respectively) established the *R*-configuration at C-13 and consequently allowed assignment of the complete stereostructure of **2** as (3*R*,9*E*,11*E*,15*E*)-13-Hydroxy-9,11,15-octadecatrienoic acid.

In briefly, α-Linolenic acid is the most abundant octadecatrienoicacid in the nature, has C=C at C9, C-12 and C-15 [20]. As a relevant of mono-hydroxy octadecatrienoic acids from natural source, 2-hydroxy-9,12,15-triene, 2-hydroxylinolenic acid ‹from the seed oil of *Thymus vulgaris* [21], 18-hydroxy-9,11,13-triene, kamlolenic acid, from the seeds of *Mallotus discolor* [22], (ζ)-3-hydroxy-octadeca-4(*E*),6(*Z*)-dienoic acid [17] and 13-hydroxy-9*Z*,11*E*,15*E*-octadecatrienoic acid [19], derivatives have been previously reported. In addition to the two stereoisomers of our dealing compounds **1**,**2** which was defined as (3*R*,4*E*,6*E*)-3-Hydroxy-4,6-octadecadienoic acid (**1**) and (3*R*,9*E*,11*E*,15*E*)-13-Hydroxy-9,11,15-octadecatrienoic acid (**2**). If we relied merely on optical rotations for stereochemical determination, and coupling constants of the chital centre, we would have made an erroneous assignment at C-3 for **1** and C-13 for **2**. Also, Most of UHFAs are not have a high degree of stability. So, if UHFAs have a degree of stability, we recommend the advantageof upgrading the configurationto the absolute one, through application of the Mosher methods. Knowledge of these advantages and drawbacks of each of these techniques will help the analyst to estimate the results published in literature at their true values. The present study established *Styrex benzoin* as a potential source of anti-inflammatory phytochemicals such as compound **2**.

4. Conclusions

The current concept of this study is one of the plant aspects of unsaturated lipids. Both of the two newly phospholipids are the classical example of a chain length of 18 carbons which are the most abundant unsaturated fatty acids in nature with the presence of a carbinolic center besides an *E*-orientation of the stereocenters. The importance of understanding the stereochemistry of the chirality active center and regiospecific double bond position in C18 unsaturated hydroxy fatty acids promotes the chemistry of fatty acids. Understanding the stereochemistry of hydrogen removal as it relates to enantioselectivity of hydrogen removal (pro *R* or pro *S*) at the prochiral methylene centres and the relative stereochemistry of C–H bond breakage at the adjacent carbons (*syn* vs *anti*) is like ly to open new doors in the biosynthesis. Compound **2**'s potent anti-inflammatory properties suggest that it could be developed further as an anti-inflammatory candidate (**Figure 7**).

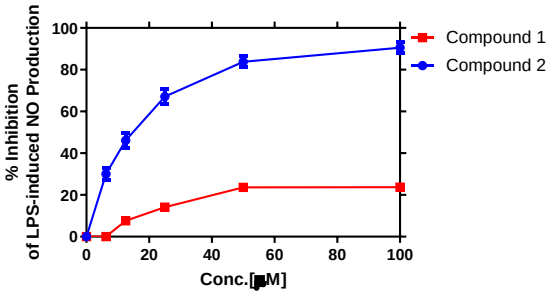

Figure 7. Concentration-dependent inhibition of LPS-activated NO release from RAW264.7 cells. Macrophages were treated for 24 h with compound **1** or **2** in the presence of 100 ng/ml LPS at the indicated concentrations. Griess assay was used to measure NO inhibition as detailed in the methods section. Data are mean±SEM.

5. Conflicts of interest

Authors declare no interests.

6. Acknowledgements

Authors acknowledge National Research Centre for supporting research facilities.

7. References

[1] Yue GW, Young O, and Fereidoon S. Chemistry of Fatty Acids. *Bailey's Industrial Oil* and *Fat Products*, Seventh Edition, John Wiley & Sons, Ltd (2020).

[2] Peter HB. Unsaturated Fatty Acids. *Comprehensive Natural Products II*, **1**, 5–33 (2010).

[3] Ledoux M, Laloux L, and Wolff RL. Analytical methods for determination of *trans*-C18 fatty acid isomers in milk fat. *Analusis*, **28**, 402-412 (2000).

[4] Abd El-Razek MH. Triterpenes from *Styrax benzoin*. *Der Pharma Chemica*, **10**, 30-34 (2018).

[5] Furman D, Campisi J, Verdin E, Carrera-Bastos P,Targ S, Franceschi C, Ferruccl L, Gilroy DW, Fasano A, Miller GW, Miller AH, , Mantovani A, Weyand CM, Barzilai N, Goronzy JJ, Rando TA, Effros RB, Lucia A, Kleinstreuer N, and Slavich GM. Chronic inflammation in the etiology of disease across the life span. *Nature Medicine*, **25**, 1822-1832 (2019).

[6] Sharif A, Nawaz H, Rehman R, Mushtaq A, and Rashid U. A review on bioactive potential of *Benzoin* Resin. *Inter. J. Chem. and Biochem. Sci.***10**, 106-110 (2016).

[7] Tanaka T, Hosokawa M, Yasui Y, Ishigamori R, and Miyashita K. Cancer Chemopreventive Ability of Conjugated Linolenic Acids. *Int. J. Mol. Sci.* **12**, 7495-7509 (2011).

[8] Hamed AR, EL-Hawary SS, Ibrahim RM, Abdelmohsen UR, EL-Hawany AM, and Alawany, A.M. Identification of Chemopreventive Components from Halophytes Belonging to Aizoaceae and Cactaceae Through LC/MS-Bioassay Guided Approach. *J. Chromatogr. Sci.* **59**, 618-626 (2021).

[9] Oliveira T, Figueiredo CA, Brito C, Stavroullakis A, Prakki A, Da Silva Velozo E, and Nogueira-Filho G. Effect of *Allium cepa* L. on Lipopolysaccharide-Stimulated Osteoclast Precursor Cell Viability, Count, and Morphology Using 4',6-Diamidino-2-phenylindole-Staining. *Int. J. Cell. Biol.* 2014, 535789 (2014).

[10] Mossob MM, Milosevic V, Milosevic M, Kramer JKC, and Azizian H. Determination of total *trans* fats and oils by infrared spectroscopy for regulatory compliance. *Anal. Bioanal. Chem.*, **389**, 87–92 (2007).

[11] Chisholm MJ, and Hopkins CY. Conjugated fatty acids in some Cucurbitaceae seed oils. *Can. J. Biochem.* **45**, 1081–1086 (1967).

[12] Hopkins CY, and Chisholm MJ. Isolation of natural isomer of linoleic acid from seed oil. *J. Am. Oil Chem. Soc.* **41**, 42–44 (1964).

[13] Breithaupt ED. Identification and Quantification of Astaxanthin Esters in Shrimp (*Pandalus borealis*) and in a Microalga (*Haematococcus pluvialis*) by Liquid Chromatography−Mass Spectrometry Using Negative Ion Atmospheric Pressure Chemical Ionization. *J. Agric. Food Chem.*, **52**, 3870−3875 (2004).

[14] Hsu F-F, Jiang X, and Frankfater C. Characterization of Long-Chain Fatty Acid As N-(4-Aminomethylphenyl) Pyridinium Derivative by MALDI LIFT-TOF/TOF Mass Spectrometry. *J. Am. Soc. Mass Spectrom.* **29**, 1688–1699 (2018).

[15] Yang K, Dilthey GB, and Gross WR. Identification and Quantitation of Fatty Acid Double Bond Positional Isomers: A Shotgun Lipidomics Approach Using Charge-Switch Derivatization. *Anal. Chem.*, **85**, 9742−9750 (2013).

[16] Black AB, Sun C, Zhao YY, Ganzle GM and Curtis JM. Antifungal Lipids Produced by Lactobacilli and Their Structural Identification by Normal Phase LC/Atmospheric Pressure Photoionization−MS/MS. *J. Agric. Food Chem.*, **61**, 5338−5346 (2013).

[17] Stavri M, Mathew KT, and Gibbons S. Antimicrobial constituents of *Scrophulariadeserti*. *Phytochemistry* **67**, 1530–1533 (2006).

[18] Ohtani, I, Kusumi T, Kashman Y, and Kakisawa H. High-field FT NMR application of Mosher's method. The absolute configurations of marine terpenoids. *J. Am. Chem. Soc*, **113**, 4092-4096 (1991).

[19] Bang M-H, Han J-T, Kim HY, Park Y-D, Park C-H, Lee K-R, and Baek N-I. 13-Hydroxy-9*Z*,11*E*,15*E*-octadecatrienoic Acid from the Leaves of *Cucurbita moschata*. *Arch. Pharm. Res*. **25**,438-440 (2002).

[20] Chisholm MJ. And Hopkins CY. Fatty Acids of *Catalpabignonioides* and Other Bignoniaceae Seed Oils. *Can. J.Chem.*. **43**, 2566-2570 (1965).
[21] Smith Jr CR, and Wolff, I. Characterization of Naturally Occurring α–Hydroxylinolenic Acid. *Lipids*, **4**, 9-14 (1968).
[22] Hopkins CY, Chisholm MJ, and Ogrodnik, JA. Identity and Configuration of Conjugated Fatty Acids in Certain Seed Oils. *Lipids*, **4**, 89-92 (1986).